1 **Heterogeneity of proteome dynamics between connective tissue phases of**
2 **adult tendon**

3 Deborah Simpson[1#], Howard Choi[2#], Ding Wang[2], Mark Prescott[1], Andrew A. Pitsillides[3],
4 Jayesh Dudhia[4], Peter D. Clegg[5], Peipei Ping[2], Chavaunne T. Thorpe[3*]

5 [1]Centre for Proteome Research, Biosciences Building, Institute of Integrative Biology,
6 University of Liverpool, Crown Street, Liverpool, L69 7ZB, UK

7 [2]Department of Physiology and Medicine, David Geffen School of Medicine, UCLA, Los
8 Angeles, CA 90095, USA

9 [3]Department of Comparative Biomedical Sciences, Royal Veterinary College, Royal College
10 Street, London, NW1 0TU, UK

11 [4]Department of Clinical Sciences and Services, Royal Veterinary Collage, Hawkshead Lane,
12 Hatfield, AL9 7TA, UK

13 [5]Department of Musculoskeletal Biology, Institute of Ageing and Chronic Disease,
14 University of Liverpool, Liverpool, West Derby Street, Liverpool, L7 8TX, UK

15

16 [#]These authors contributed equally to this study

17 [*]Corresponding Author: cthorpe@rvc.ac.uk

18

19 Declarations of interest: none

20

1   **Abstract**

2   Maintenance of connective tissue integrity is fundamental to sustain function, requiring

3   protein turnover to repair damaged tissue. However, connective tissue proteome dynamics

4   remain largely undefined, as do differences in turnover rates of individual proteins in the

5   collagen and glycoprotein phases of connective tissue extracellular matrix (ECM). Here, we

6   investigate proteome dynamics in the collagen and glycoprotein phases of connective tissues

7   by exploiting the spatially distinct fascicular (collagen-rich) and interfascicular (glycoprotein-

8   rich) ECM phases of tendon. Using isotope labelling, mass spectrometry and bioinformatics,

9   we calculate turnover rates of individual proteins within rat Achilles tendon and its ECM

10 phases. Our results demonstrate complex proteome dynamics in tendon, with ~1000-fold

11 differences in protein turnover rates, and overall faster protein turnover within the

12 glycoprotein-rich interfascicular matrix compared to the collagen-rich fascicular matrix.

13 These data provide insights into the complexity of proteome dynamics in tendon, likely

14 required to maintain tissue homeostasis.

15 **Keywords:** Tendon; proteome dynamics; deuterium; interfascicular matrix; proteomics,
16 proteostasis

17

Introduction

Maintaining the structural and mechanical integrity of tissues in the musculoskeletal system, and other connective tissues, is fundamental to sustain tissue homeostasis and healthy function, requiring protein synthesis and degradation to repair and/or replace damaged tissue before damage accumulates and leads to injury (Humphrey et al., 2014). However, while the composition and structure of connective tissues is well defined (Scott, 1983), relatively little is known regarding proteome dynamics in connective tissues, particularly at the level of the individual constituent proteins.

Connective tissues consist of fibrous proteins (predominantly collagen) embedded in a glycoprotein-rich matrix (Scott, 1983), and variation in the organisation of both phases give rise to tissues with distinct structural and mechanical properties (Culav et al., 1999). Research in a variety of tissues including skin, tendon and cartilage indicates a relatively long half-life of collagens, with more rapid turnover of glycoproteins and other non-collagenous proteins (Thorpe et al., 2010, Maroudas et al., 1998, Sivan et al., 2006, Sivan et al., 2008, Verzijl et al., 2000). Indeed, several studies have reported negligible turnover of collagen, the major component of tendon and other connective tissues, within an individual's lifetime (Thorpe et al., 2010, Heinemeier et al., 2013, Heinemeier et al., 2016). However other studies have measured relatively rapid collagen synthesis in tendon, both at basal levels and in response to exercise (Miller et al., 2005), and also identified soluble collagen with a much shorter half-life compared to the majority of collagen in human articular cartilage (Hsueh et al., 2019); the location(s) of these more labile proteins remain to be identified. When taken together, these contradictory findings indicate that proteome dynamics in connective tissues is complex, and that the glycoprotein-rich phase may be replenished more rapidly than the collagen-rich phase. However, the turnover rate of individual proteins within the different phases of the

1 extracellular matrix (ECM), and the potential contribution of differential regulation of protein

2 turnover to maintenance of tissue homeostasis remain undefined.

3 Tendon provides an ideal model in which to separately interrogate protein turnover in these

4 ECM phases, as it consists of highly aligned, collagen-rich fascicular matrix (FM),

5 interspersed by a less dense glycoprotein-rich phase, termed the interfascicular matrix (IFM,

6 also referred to as the endotenon) (Kastelic et al., 1978). While the FM is predominantly

7 composed of type I collagen, glycoproteins are also present in this region at low abundance

8 (Thorpe et al., 2016b). Similarly, the IFM contains small amounts of a variety of collagens

9 (Södersten et al., 2013, Thorpe et al., 2016b). Due to the highly aligned structure of tendon

10 tissue, it is possible to separate FM and IFM for individual analysis using laser capture

11 microdissection (Thorpe et al., 2016b, Zamboulis et al., 2018). Indeed, these, and other

12 studies, have shown greater expression of markers of ECM degradation, as well as increased

13 neo-peptide levels, a proxy measure of protein turnover, within the IFM (Spiesz et al., 2015,

14 Thorpe et al., 2015a, Thorpe et al., 2016b), suggesting this region is more prone to

15 microdamage, likely due to the high shear environment that occurs due to interfascicular

16 sliding (Thorpe et al., 2012, Thorpe et al., 2015b). Taken together, these findings suggest that

17 there is greater turnover of ECM proteins localised to the IFM than within the FM to repair

18 local microdamage and maintain tendon homeostasis.

19 Due to a lack of available methodology, it has not been possible until recently to study

20 differential rate of turnover at the individual protein level. However, novel bioinformatics

21 software developments, in combination with in vivo isotope labelling, and mass spectrometry

22 technologies, now provide the capacity to determine the turnover rates of individual proteins

23 within a sample (Kim et al., 2012, Lam et al., 2014, Lau et al., 2016). The aim of this study is

24 therefore to apply this technique to tendon, firstly to establish the proteome-wide turnover

25 rate of tendon, and secondly to combine this approach with laser capture microdissection to

1   test the hypothesis that the proteome of the IFM is more dynamic than in the FM, with faster

2   turnover of individual proteins. More rapid remodelling of the IFM would provide a

3   mechanism by which shear-induced microdamage to this region could be repaired, preventing

4   damage accumulation and subsequent injury.

5   **Results**

6   *²H enrichment in serum water* – In rats labelled with deuterium over a period of 127 days

7   (Fig. 1a), ²H enrichment of serum occurred rapidly and in a similar manner to that reported

8   previously in rodents (Kim et al., 2012), reaching a plateau of 5.6% by day 4, and remained

9   constant throughout the study (Fig. 1b). The enrichment curve, which was empirically

10   derived from the GC-MS measurements at the sampled time points, defines two parameters:

11   deuterium enrichment rate (k_p) = 0.7913 and plateau (p_{ss}) = 0.0558; these values were used

12   for subsequent kinetic curve fitting to calculate peptide turnover rate constants (k).
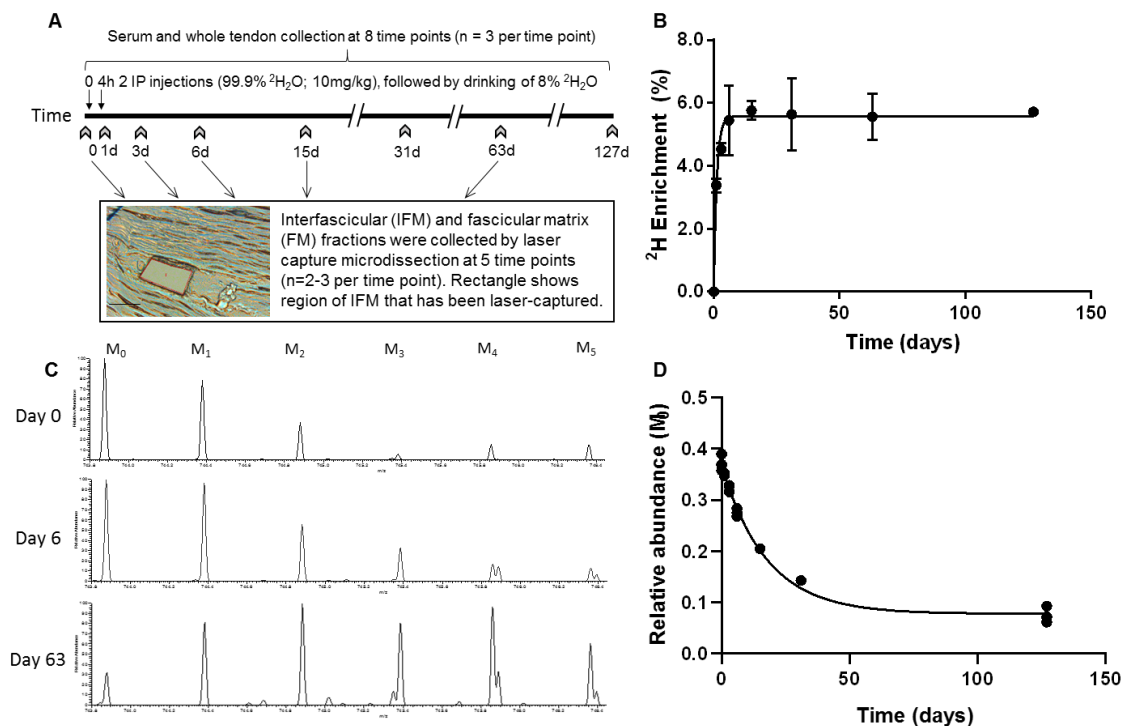
13

14   **Figure 1. Metabolic labelling of rats using deuterium**. *A,* Schematic showing ^2H_2O

15   labelling of rats and details of sample collection, and interfascicular matrix isolation by laser

5

1   capture microdissection (scale bar = 100µm). *B,* ^{2}H enrichment in serum occurred rapidly,

2   reaching a plateau of 5.6 % by day 4 and remained constant throughout the study. Data are

3   shown as mean ± SD and raw data provided in source table 1. *C,* Example extracted ion

4   chromatograms from tendon samples demonstrating increased abundance of higher mass

5   isotopomer peaks over the course of the study ($M_1 – M_5$). *D,* Example curve showing the

6   relative abundance of the unlabelled monoisotopic peak (M_0) for the cartilage oligomeric

7   matrix protein (COMP) peptide QMEQTYWQANPFR, calculated by ProTurn software and

8   plotted as a function of time.

9

10 *Protein Identification* – 155 proteins with ≥2 unique peptides were identified in whole tendon

11 digests and are shown in supplementary table 1. Of these proteins, 67 were classified as ECM

12 or ECM-related proteins by MatrisomeDB (Hynes and Naba, 2012). In samples collected by

13 laser capture microdissection of tendon cryosections, 243 proteins with ≥2 unique peptides

14 were identified in the IFM, 70 of which were ECM or ECM-related proteins (Supplementary

15 table 2). In the FM, 98 proteins were identified, of which 55 were ECM or ECM-related

16 proteins (Supplementary table 3). Protein interactions for each tendon component are shown

17 in supplementary figure 1, demonstrating a complex and highly interconnected proteome in

18 tendon and its ECM phases.

19 *Protein Turnover in whole tendon* – Peptide turnover rates were calculated using ProTurn

20 (v2.1.05; http://proturn.heartproteome.org; (Lam et al., 2014, Lau et al., 2016, Lau et al.,

21 2018, Wang et al., 2014)), which automatically calculates turnover rate constants for all

22 peptides that pass the selection criteria using non-steady state curve fitting (Fig. 1). To assure

23 data quality, we used a stringent cut-off, passing only peptides that are identified at 1% false

24 discovery rate (FDR) and quantified at 4 or more time points. In total, 179 peptides, relating

1   to 39 proteins, passed the ProTurn selection criteria and were used to calculate protein half-

2   life in whole tendon samples.
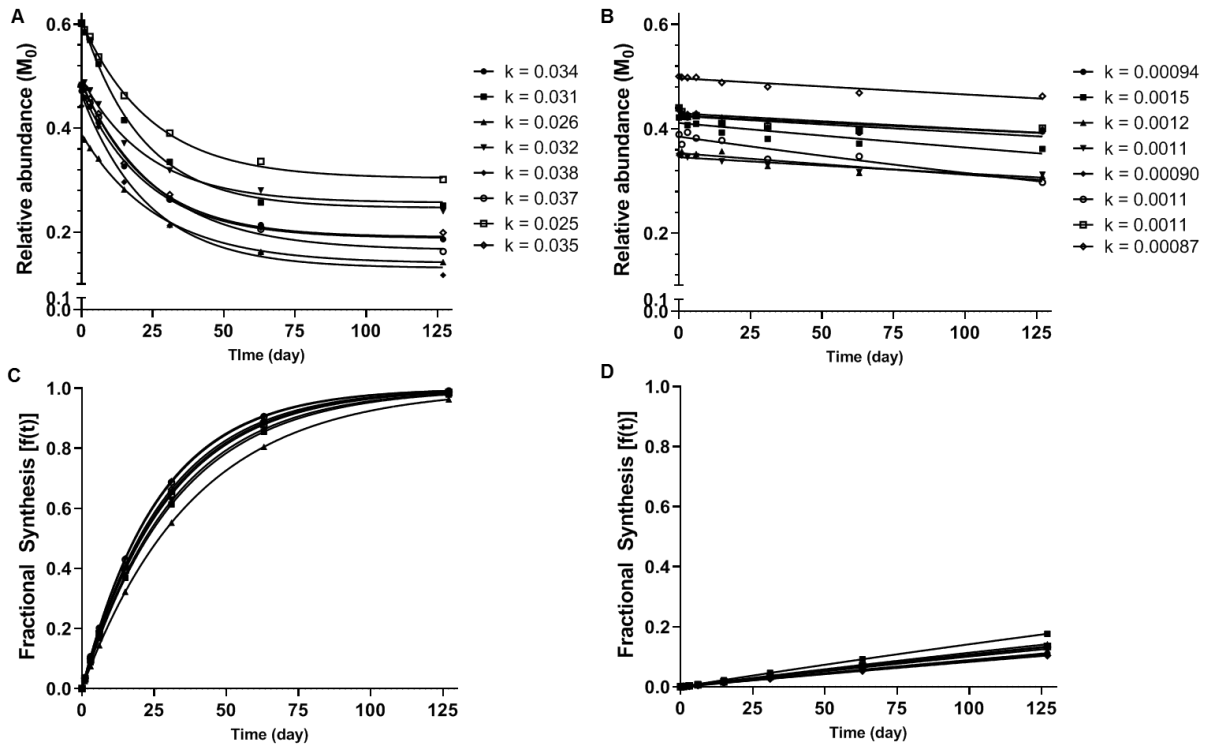
3

4   **Figure 2. Calculation of protein turnover rate from mass isotopomer distribution over**

5   **time.** Relative abundance of M_0 in selected decorin (*A*) and collagen type 1, alpha 1 chain (*B*)

6   peptides, and resulting *k* values calculated by non-steady state curve fitting using ProTurn

7   software. Fractional synthesis rates (FSR), calculated from peptide *k* values, demonstrate

8   more rapid turnover of decorin (*C*) compared to collagen type 1, alpha 1 chain (*D*). Source

9   data, generated by ProTurn are available in source table 2.

10

11   The relative abundance of the unlabelled monoisotopic peak (M_0), plotted as a function of

12   time for selected decorin and collagen peptides are shown in Fig. 2a&b. Non-steady state

13   curve fitting was performed by ProTurn to calculate turnover rate constants (*k*) for each

14   peptide, and resultant fractional synthesis curves in Fig. 2c&d demonstrate much faster

7

1   turnover of decorin peptides compared to collagen types 1 and 3. *k* values for all peptides

2   identified, and corresponding protein half-lives are shown in Fig. 3. As expected, the smallest

3   *k* values related to collagenous proteins, with corresponding half-lives of 508 to 756 days. By

4   contrast, the protein identified with the fastest turnover was the glycoprotein clusterin, with a

5   half-life of 1.4 days. The half-life of proteoglycans ranged from 21 days for decorin to 72

6   days for lumican. With the exception of collagens, which all exhibited low turnover rates,

7   there was no clear relationship between protein class and rate of turnover (Fig. 3c).
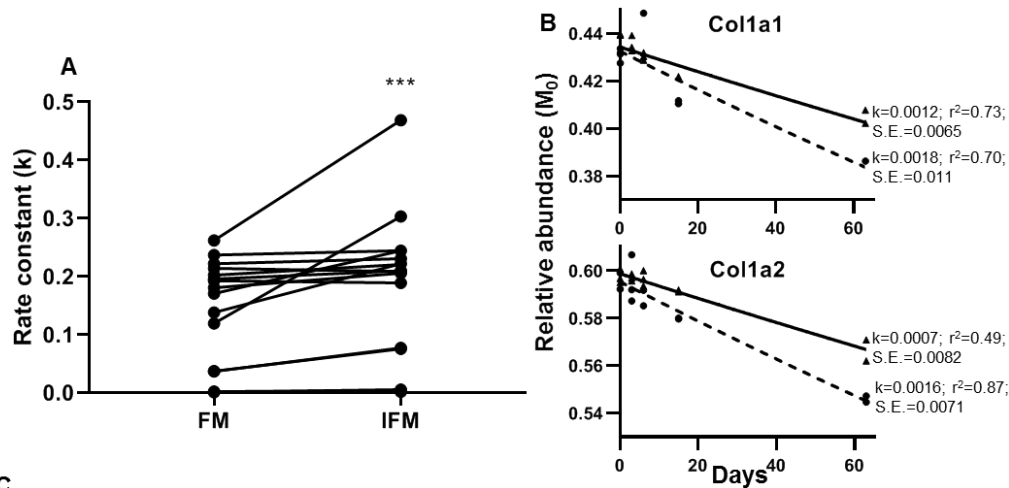

8
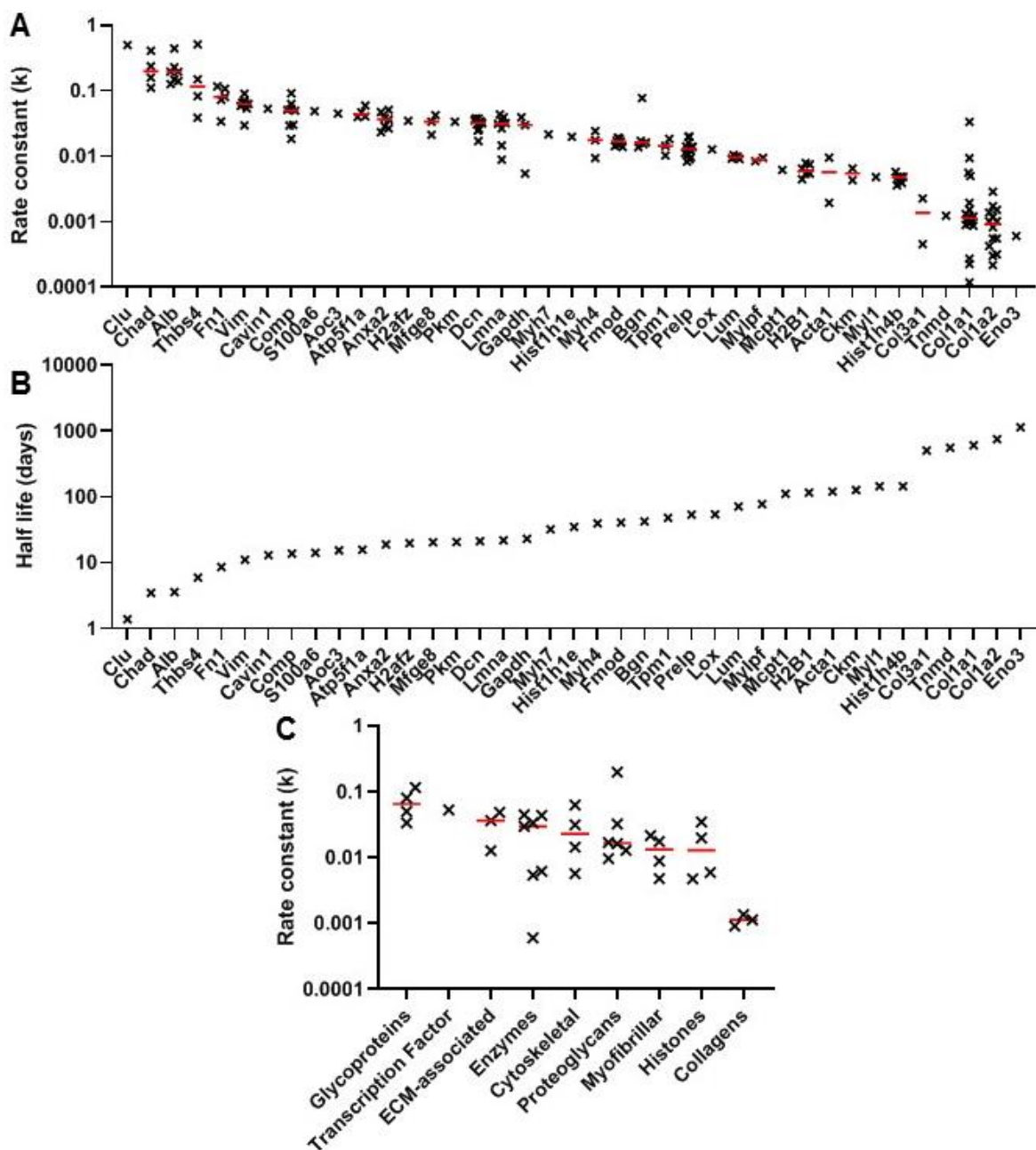
1   **Figure 3. Peptide turnover rate constants and corresponding protein half-lives in whole**

2   **tendon.** *A*, the peptide rate constants *(k)* for individual proteins are plotted in descending

3   order on a logarithmic scale, with the median value represented by a red line. *B*, the median *k*

4   values for each protein were used to calculate protein half-life, assuming a first order

5   reaction. *C,* protein turnover rates plotted against MatrisomeDB and PANTHER categories,

6   with the median value represented by a red line. Due to space constraints, gene, rather than

7   protein, names are displayed in parts *A* and *B*. Source data, generated by ProTurn are

8   available in source table 2.

9

10   *Protein turnover in tendon compartments* −91 peptides, relating to 18 proteins, and 39

11   peptides, relating to 11 proteins, passed the ProTurn selection criteria in the FM and IFM

12   respectively. 23 peptides were present both in the IFM and FM, and *k* values were

13   significantly greater for these peptides in the IFM compared to the FM (Fig. 4a),

14   demonstrating an overall faster rate of protein turnover in the IFM. The turnover rate

15   constants and resultant half-lives for proteins identified in each tendon phase are shown in

16   Fig. 4b. Turnover rate constants for collagenous proteins were significantly higher in the IFM
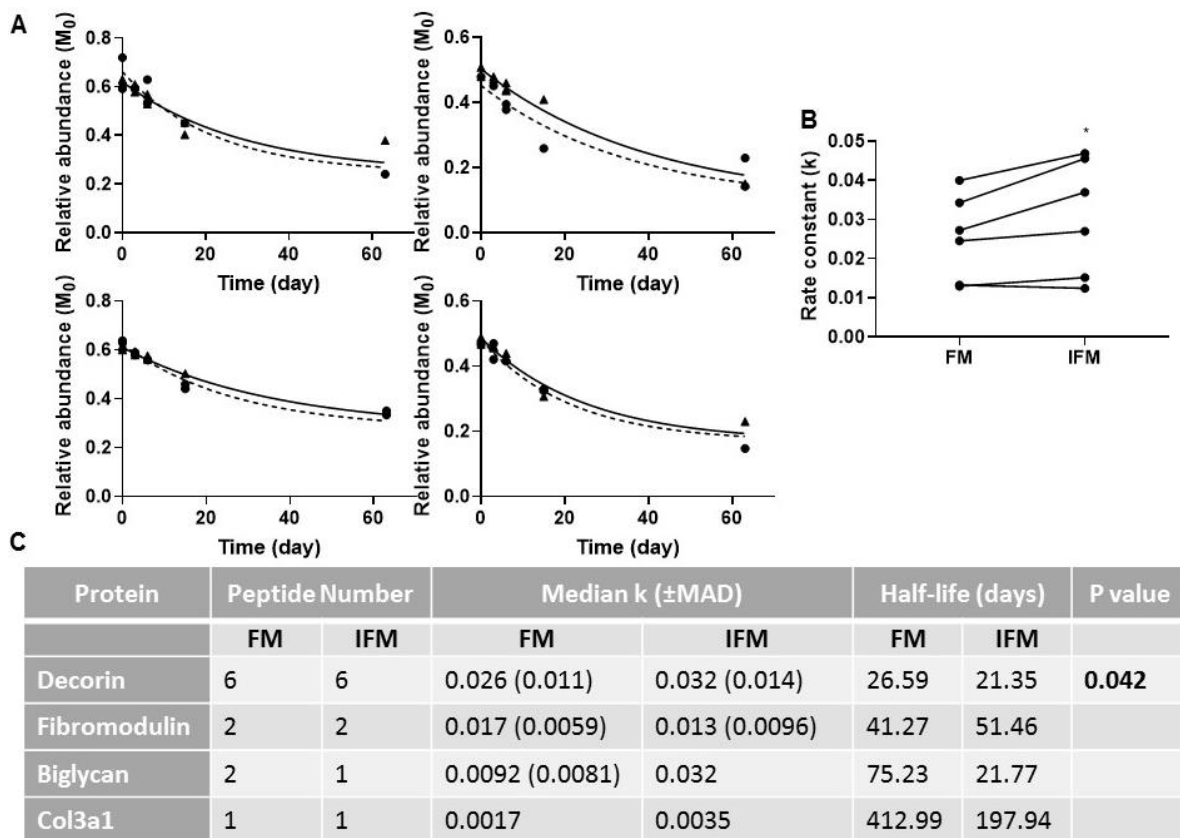
17   compared to the FM.

Figure 4. Peptide turnover rate constants and corresponding protein half-lives in tendon phases. *A,* rate constants *(k)* for peptides identified in both tendon phases were significantly greater in the IFM compared to the FM. *B,* median peptide decay curves for Col1a1 and Col1a2 in the FM (▲; solid line) and IFM (●; dashed line), showing goodness of fit (r^2) and standard error (S.E.). *C,* turnover rate constants *(k)* and corresponding half-lives

Protein	Peptide Number		Median k (±MAD)		Half-life (days)		P value
	FM	IFM	FM	IFM	FM	IFM	
Collagen type I α-1 chain	12	4	0.0012 (0.00056)	0.0018 (0.00016)	568.97	383.93	**0.042**
Collagen type I α-2 chain	12	7	0.00075 (0.00036)	0.0016 (0.00044)	925.85	421.28	**0.016**
Serotransferrin	5	3	0.26 (0.16)	0.47 (0.017)	2.64	1.53	0.26
Serum Albumin	14	12	0.20 (0.017)	0.23 (0.018)	3.50	3.11	0.051
Vimentin	4	3	0.061 (0.023)	0.084 (0.0080)	11.34	8.24	0.31
Prelamin-A/C	2	3	0.035 (0.0025)	0.043 (0.0067)	19.84	18.45	
Annexin A2	1	3	0.056	0.056 (0.0071)	12.35	12.39	
Cartilage oligomeric matrix protein	10	-	0.082 (0.0018)		8.42		
Decorin	4	-	0.039 (0.0029)		17.63		
Fibromodulin	6	-	0.022 (0.0026)		33.27		
Fibronectin	3	-	0.10 (0.0099)		6.63		
Gelsolin	2	-	0.52 (0.17)		1.32		
Prolargin	3	-	0.015 (0.00031)		46.30		
Thrombospondin-4	3	-	0.068 (0.0037)		10.18		
Hemoglobin subunit alpha-1/2	-	2		0.024 (0.0021)		29.06	
Anionic trypsin-1	1	-	0.00036		1946.63		
Biglycan	1	-	0.010		66.71		
Chondroadherin	1	-	0.63		1.10		
Glyceraldehyde-3-phosphate dehydrogenase	1	-	0.029		23.79		
Fatty acid-binding protein, adipocyte	-	1		0.12		5.65	
Hemoglobin subunit beta-1	-	1		0.031		22.28	
Mast cell protease 1	-	1		0.010		69.15	

10

1   for proteins identified in each phase. *** indicates p < 0.0001. Source data, generated by

2   ProTurn are available in source tables 3 and 4.

3

4   Due to ProTurn software identifying a low number of proteins in laser captured samples,

5   particularly in the IFM, turnover rate constants in tendon phases were calculated manually for

6   a number of proteins of interest (Fig. 5). Rate constants of turnover of decorin peptides were

7   significantly higher in the IFM compared to the FM (Fig. 5). It was not possible to assess

8   differences in turnover of other proteins due to a low number of peptides identified at

9   sufficient time points to allow accurate curve fitting (Fig. 5c).

Protein	Peptide Number		Median k (±MAD)		Half-life (days)		P value
	FM	IFM	FM	IFM	FM	IFM	
Decorin	6	6	0.026 (0.011)	0.032 (0.014)	26.59	21.35	**0.042**
Fibromodulin	2	2	0.017 (0.0059)	0.013 (0.0096)	41.27	51.46	
Biglycan	2	1	0.0092 (0.0081)	0.032	75.23	21.77	
Col3a1	1	1	0.0017	0.0035	412.99	197.94	

10

11   **Figure 5. Manual calculation of turnover rate of selected proteins.** *A*, Relative abundance

12   of M_0 as a function of time, and resultant non-linear curve fitting for peptides corresponding

13   to decorin identified in the FM (▲; solid line) and IFM (●; dashed line). *B*, resultant *k* values

11

1   for decorin peptides were significantly greater in the IFM than in the FM (p = 0.042). *C*,

2   manually calculated turnover rate constants *(k)* and corresponding half-lives for tendon

3   proteins of interest.

4

5   **Discussion**

6   This is the first study to investigate the proteome-wide turnover rate of tendon and its

7   constituent ECM phases, demonstrating complex proteome dynamics in whole tendon.

8   Protein turnover rate in tendon varied almost 1000-fold, with half-lives ranging from 1.5 days

9   to over 1000 days. The results also support our hypothesis, demonstrating significantly faster

10   turnover of proteins in the glycoprotein-rich IFM compared to the collagen-rich FM, both

11   overall and when directly comparing individual proteins.

12   In agreement with previous studies (Thorpe et al., 2016b), the IFM had a more complex

13   proteome than the FM, with a greater number of proteins identified in this region. Indeed,

14   more proteins were identified within the IFM than in whole tendon samples; this is likely due

15   to the predominance of collagen in whole tendon samples which precludes detection of

16   proteins present at lower abundance in these samples. As many of the proteins present in the

17   IFM were identified in less than 4 samples, it was not possible to perform curve fitting to

18   calculate the turnover rate for these proteins. Due to the small size of the rat Achilles tendon,

19   it was not possible to laser-capture a larger volume of IFM, and pooling samples from each

20   time point for LC-MS/MS analysis did not result in a greater number of protein hits than

21   when each sample was analysed separately. In addition, it was necessary to calculate turnover

22   rates of some proteins manually as automated identification of isotopomer peaks was

23   unsuccessful, particularly in IFM samples. While turnover rates calculated manually cannot

24   be compared directly to those calculated automatically by ProTurn, due to differences in

1   curve fitting, it is possible to compare turnover rates of IFM and FM proteins, where both are

2   calculated manually. Despite these limitations, results reveal a diverse rate of protein turnover

3   in both the FM and IFM, with values for individual proteins similar to those observed when

4   the tendon matrix was analysed as a whole.

5   Collagenous proteins had the slowest turnover of all tendon matrix proteins identified, in the

6   whole tendon, and in the FM and IFM, with a half-life from approximately 1 year in the IFM

7   to 3 years in the FM. While relatively slow, this contrasts with previous studies which have

8   reported that collagen is essentially inert in the adult rat patellar tendon (Bechshøft et al.,

9   2017) and in tendons from larger animals (Heinemeier et al., 2013, Thorpe et al., 2010), as

10   well as in cartilage and intervertebral disc (Heinemeier et al., 2016, Sivan et al., 2008).

11   However, these previous studies have either analysed tissues as a whole, or separated the

12   tissue into collagenous and non-collagenous fractions, rather than calculating turnover of

13   individual proteins, such that they lack the specificity achieved by using deuterium labelling

14   combined with mass spectrometry analysis. Other studies that have measured collagen

15   synthesis in human tendon using stable isotope labelling and performing tendon biopsies,

16   report contradictory findings, calculating a FSR of $0.04 - 0.06\%$ hour^{-1}, which equates to a

17   half-life ranging from 48 to 64 days (Miller et al., 2005, Babraj et al., 2005, Smeets et al.,

18   2019). However, these were very short term studies, and it is unlikely that all newly

19   synthesised protein would be incorporated into the matrix, such that FSR is over-estimated

20   (Heinemeier et al., 2013). The results we present here help to explain these apparent

21   contradictory findings, suggesting that the pool of more labile collagen identified previously

22   in human tendon and cartilage (Miller et al., 2005, Hsueh et al., 2019) may be located in the

23   glycoprotein-rich ECM phase rather than with the bulk of the fascicular collagen.

24   In addition, it is likely that overall protein turnover rate is more rapid in small compared to

25   large animals. While few studies have directly compared protein turnover kinetics between

1   species, a recent study of protein turnover in dermal fibroblasts from different rodent species

2   demonstrated a negative correlation between median k values and lifespan (Swovick et al.,

3   2018). In support of this, the half-life of serum albumin is approximately 10 fold greater in

4   the human compared to the rat (Chaudhury et al., 2003, Jeffay, 1960). Taken together, it can

5   be presumed that turnover of tendon ECM proteins is also likely slower in larger animals than

6   those we report here for the rat, but the relative differences observed between individual

7   proteins and ECM phases are likely to persist in humans and other large animals.

8   It is also important to recognise that specific proteins that are not core components of the

9   tendon ECM will not be metabolised within the tendon, but instead will be synthesised

10   elsewhere and transported to the tendon via the circulation. Specifically, serum albumin and

11   serotransferrin are predominantly synthesised and secreted by the liver (Tavill, 1972),

12   whereas haemoglobin is synthesised in the bone marrow and its turnover provides a measure

13   of erythrocyte lifespan (Koury, 2016).

14   The measured rate constants of protein turnover will also be dependent on the protein

15   extraction methods used. We chose GuHCl extraction for whole tendon as this has previously

16   been shown to result in best proteome coverage for tendon (Ashraf Kharaz et al., 2017). It

17   was not possible to use the same extraction method for laser-captured samples due to the

18   small amount of starting material, therefore we used a method previously optimised for this

19   sample type (Thorpe et al., 2016b). Despite differences in extraction techniques used, protein

20   half-lives were similar in the whole tendon and the fascicular matrix, suggesting minimal

21   effects from using different extraction techniques. Indeed, previous studies, in which the rat

22   Achilles was acid-solubilised post deuterium labelling and FSR measured by GC-MS,

23   reported a FSR of 0.66 % day[-1] (Katsma et al., 2017) which equates to a half-life of 105 days,

24   supporting the results we present here, in which average protein half-life in whole tendon is

25   131 days.

1   As well as providing the first data on individual protein turnover rates in tendon, this work

2   builds on our understanding of the role of the IFM in tendon function. Previous work has

3   shown that the IFM has specialised composition and function, facilitating sliding between

4   tendon fascicles to provide extensibility to the tendon (Thorpe et al., 2012, Thorpe et al.,

5   2015b, Thorpe et al., 2016b, Thorpe et al., 2016c, Thorpe et al., 2016a). Cyclic sliding and

6   recoil increases the risk of microdamage to this region (Spiesz et al., 2015), and therefore

7   greater turnover of IFM proteins may be a protective mechanism to repair this damage. We

8   have previously demonstrated that elastin and lubricin are localised to the IFM and likely

9   contribute to its mechanical function (Godinho et al., 2017, Thorpe et al., 2016a). However,

10   these proteins are difficult to identify using LC-MS/MS (Thorpe et al., 2016b) so we were

11   unable to assess their rate of turnover.

12   We extend previous observations in tendon and other musculoskeletal tissues (Thorpe et al.,

13   2010, Sivan et al., 2006, Maroudas et al., 1998, Hsueh et al., 2019), measuring considerably

14   faster turnover of proteoglycans compared to collagens in tendons, FM and IFM.

15   Interestingly, there were variations in rates of small leucine-rich proteoglycan turnover

16   between tendon phases. Significantly faster turnover of decorin was observed in the IFM

17   compared to the FM, whereas the results suggest that faster fibromodulin turnover may occur

18   within the FM. Indeed, previous studies have shown a greater abundance of fibromodulin in

19   the FM compared to the IFM (Thorpe et al., 2016b, Thorpe et al., 2016a). While the role of

20   different proteoglycans in modulating collagen fibrillogenesis during tendon development is

21   well defined (Connizzo et al., 2013), their roles in the function of mature tendon are less well

22   characterised. Recent work using decorin and biglycan inducible knock-out mice

23   demonstrated alterations in collagen fibril diameter and decreased tendon mechanical

24   properties in the adult, indicating an important role for these proteoglycans in FM and

25   subsequently, tendon homeostasis (Robinson et al., 2017). It is likely that proteoglycans also

1   contribute to homeostasis within the IFM, but the roles of specific proteins in the IFM during

2   development and in the adult remain to be defined.

3   Our results show that proteome dynamics in tendon is highly complex, with differences in

4   protein-selective turnover rates observed in distinct IFM and FM ECM phases. Regulation of

5   protein turnover is multifactorial, involving pathways controlling protein synthesis, folding,

6   transport, assembly, disassembly, and degradation (Powers et al., 2009). Recent studies have

7   identified the important role of transforming growth factor-β (TGF-β) in regulating ECM

8   remodelling in tendon and other tissues (Gumucio et al., 2015, Rys et al., 2016). Indeed, it

9   has been shown that TGF-β localises to the IFM in developing and adult tendon (Kuo et al.,

10   2008, Russo et al., 2015), which is consistent with the notion that increased TGF-β signalling

11   could have a role in this faster protein turnover identified in the IFM.

12   *Conclusions*

13   This is the first study to determine the turnover rate of individual proteins in different

14   connective tissue phases, demonstrating complex proteome dynamics in tendon, with an

15   overall faster turnover of proteins in the glycoprotein-rich IFM phase. Greater capacity for

16   turnover of this phase of the tendon matrix may be indicative of a mechanism that reduces the

17   accumulation of damage caused by the high shear environment within this region, although

18   this remains to be directly determined. The techniques used here provide a powerful approach

19   to interrogate alterations in connective tissue protein turnover with ageing and/or disease

20   which are likely to influence injury risk.

21   **Materials and Methods**

22   *Animals* - Female Wistar rats (n = 24, 12 week old, weight: 270 ± 18g, range: $228 - 299$g,

23   Charles River Company, UK) were housed in polypropylene cages in groups of 3, subjected

24   to 12 h light/dark cycle with room temperature at $21 \pm 2°C$ and fed ad libitum with a

1   maintenance diet (Special Diet Services, Witham UK). All procedures complied with the

2   Animals (Scientific Procedures) Act 1986, were approved by the local ethics committee at the

3   Royal Veterinary College and are reported according to the ARRIVE guidelines (Kilkenny et

4   al., 2010).

5   *In vivo isotope labelling* – All rats, with the exception of the controls (n=3) received 2

6   intraperitoneal injections of 99% $[^2H]_2O$ (10ml/kg; CK isotopes Ltd) spaced 4 hours apart,

7   and were then allowed free access to 8% $[^2H]_2O$ (v/v) in drinking water for the duration of

8   the study to maintain steady-state labelling (Kim et al., 2012). All rats were acclimatized for

9   1 week prior to commencement of the study, and monitored daily and weighed weekly

10   throughout the study; no adverse effects were observed. Rats in the control group were

11   sacrificed on day 0. Rats in the isotope labelled groups were sacrificed on day 1, 3, 6, 15, 31,

12   63 and 127 (n=3 per time point). Rats were culled at the same time of day at each time point,

13   to minimise any effect from diurnal variations. Blood was collected from each rat

14   immediately post-mortem, and allowed to clot at room temperature. Blood samples were

15   centrifuged at 1500 g for 10 min, and serum collected and stored at -20 °C prior to analysis.

16   Both Achilles tendons were harvested within 2 hours of death. The left Achilles was snap

17   frozen in n-hexane cooled on dry ice for proteomic analysis of the whole tissue, and the right

18   Achilles was embedded in optimal cutting temperature compound and snap frozen in n-

19   hexane cooled on dry ice for isolation of fascicular and interfascicular matrices (Fig. 1a).

20   *GC-MS Analysis of Serum Water* – ^2H labelling in serum was measured via gas

21   chromatography-mass spectrometry (GC-MS) after exchange with acetone and extraction

22   with chloroform as described previously (McCabe et al., 2006). 30µl extract was analysed

23   using GC-MS (Waters GCT mass spectrometer, Agilent J&W DB-17MS column (30m x

24   0.25mm x 0.25µm)). The carrier gas was helium (flow rate: 0.8 ml/min). The column

25   temperature gradient was as follows: 60°C initial, 20°C/min increase to 100°C, 1 min hold,

17

1   then 50°C/min increase to 220°C. The injection volume was 1µl and injector temperature was

2   220°C. The mass spectrometer operated in positive ion electron ionisation mode, the source

3   temperature was 180°C and the range scanned was m/z 40-600 (scan time: 0.9s). Mass

4   spectral intensities for m/z values 58 and 59 were produced by combining the mass spectra in

5   the acetone peak to create an averaged spectrum (Waters MassLynx). Serum ^{2}H enrichment

6   was calculated by comparison to a standard curve, and first order curve fitting (GraphPad

7   Prism 8) used to calculate the rate constant (k_p) and plateau (p_{ss}) of deuterium enrichment

8   (Fig. 1b).

9   *Protein extraction from whole tendon* – Left Achilles tendons were thawed, and their surface

10   scraped with a scalpel, followed by PBS washes, to remove the epitenon and any residual

11   non-tendinous tissue. Tendons were finely chopped, flash frozen in liquid nitrogen and

12   pulverised in a dismembrator (Sartorius, mikro-dismembrator U, 1800rpm, 2 mins.). Proteins

13   were extracted using previously optimised methodologies (Ashraf Kharaz et al., 2017).

14   Briefly, following deglycosylation in chondroitinase ABC, proteins were extracted in

15   guanidine hydrocholoride (GuHCl) as described previously (Kharaz et al., 2016). Protein

16   content was determined using a Pierce protein assay according to the manufacturer's

17   instructions. Samples were stored at -80°C prior to preparation for LC-MS/MS by centrifugal

18   filtration. Filter units were rinsed with 1%(v/v) formic acid and a balance volume of buffer

19   (4M GuHCl/50mM ammonium bicarbonate (ambic)) was added. A volume equivalent to

20   50µg protein was added to each filter and the samples vortexed gently. Filters were

21   centrifuged (15 min, 12500rpm, 20°C), washed with GuHCl buffer and centrifuged again.

22   Proteins were reduced by DTT incubation (8mM in 4M GuHCl, 15 min, 56°C) and then

23   centrifuged (10 min, 12500rpm). DTT was removed by washing twice with buffer as

24   described above. Proteins were alkylated with 100µl 50mM iodoacetamide in 4M GuHCl

25   solution, vortexed and incubated in the dark (20 min., room temperature). Iodoacetamide was

18

1 removed by washing twice with GuHCl buffer as described above. Buffer was exchanged to

2 ambic by 3 washes with 50mM ambic, centrifuging after each wash. 1µg trypsin in 50mM

3 ambic was added and proteins digested overnight at 37°C with mixing. Flow through was

4 collected after centrifugation and addition of 40µl 50mM ambic. The flow though was

5 combined and acidified using trifluoroacetic acid (10%(v/v)), and diluted 20-fold in

6 0.1%(v/v) TFA/3%(v/v) acetonitrile for LC-MS/MS analysis.

7 *Isolation and extraction of fascicular and interfascicular matrix proteins* – Longitudinal

8 cryosections (15µm) from the right Achilles tendons (5 time points, n=2-3/time point) were

9 adhered to membrane slides (PEN, Leica) and stored at −80°C. Sections were prepared for

10 laser capture as described previously (Thorpe et al., 2016b) and approximately 1mm^2 of FM

11 and IFM from each sample were collected into 50µl molecular biology grade H_2O (Leica

12 LMD7000; Fig. 1a). Samples were immediately frozen and stored at −80°C. Prior to

13 digestion, samples were centrifuged immediately after removal from -80°C storage. Volume

14 was adjusted to 80µl by adding 50mM ambic, and Rapigest SF (1%(v/v) in 25mM ambic,

15 Waters, UK) was added to a final volume of 0.1%(v/v). Samples were mixed (room

16 temperature, 30 min) then incubated at 60°C (1h, 450rpm). Samples were centrifuged

17 (17200g, 10 min), vortexed, then incubated at 80°C (10 min). Proteins were reduced by

18 incubating with DTT (5µL, 60mM in 25mM ambic, 10 min, 60°C) then alkylated by adding

19 5µl 178mM iodoacetamide in 25mM ambic (30 min. incubation, room temperature, in dark).

20 Trypsin (Promega Gold sequencing grade) was diluted in 25mM ambic and added at an

21 enzyme to protein ratio of 1:50 (based on estimated protein amount from tissue volume

22 collected). Digests were incubated overnight at 37°C with an enzyme top-up after 3.5h.

23 Rapigest was hydrolysed with TFA (0.5µl, 37°C, 45 min.). Digests were centrifuged

24 (17200g, 30 min.), aspirated into low-bind tubes and de-salted on stage-tips as previously

25 described (Thorpe et al., 2016b).

19

1   *LC-MS/MS analyses* - Data-dependent LC-MS/MS analyses were conducted on a QExactive

2   quadrupole-Orbitrap mass spectrometer (Williamson et al., 2016, Michalski et al., 2011)

3   coupled to a Dionex Ultimate 3000 RSLC nano-liquid chromatograph (Hemel Hempstead,

4   UK). Digest was loaded onto a trapping column (Acclaim PepMap 100 C18, 75µm x 2cm,

5   3µm packing material, 100Å) using a loading buffer of 0.1%(v/v) TFA, 2%(v/v) acetonitrile

6   in water for 7 min (flow rate: 9µl/min). The trapping column was set in-line with an

7   analytical column (EASY-Spray PepMap RSLC C18, 75µm x 50cm, 2µm packing material,

8   100Å) and peptides eluted using a linear gradient of 96.2% A (0.1%(v/v) formic acid):3.8%

9   B (0.1%(v/v) formic acid in water:acetonitrile [80:20](v/v)) to 50% A:50% B over 60 min

10   (flow rate: 300nl/min), followed by 1% A:99% B for 5 min and re-equilibration of the

11   column to starting conditions. The column was maintained at $40^{o}C$, and the effluent

12   introduced directly into the integrated nano-electrospray ionisation source operating in

13   positive ion mode. The mass spectrometer was operated in DDA mode with survey scans

14   between *m/z* 300-2000 acquired at a mass resolution of 70,000 (FWHM) at *m/z* 200. The

15   maximum injection time was 250ms, and the automatic gain control was set to 1e6. The 10

16   most intense precursor ions with charges states of between 2+ and 4+ were selected for

17   MS/MS with an isolation window of 2 *m/z* units. The maximum injection time was 100ms,

18   and the automatic gain control was set to 1e5. Peptides were fragmented by higher-energy

19   collisional dissociation using a normalised collision energy of 30%. Dynamic exclusion of

20   *m/z* values to prevent repeated fragmentation of the same peptide was used (exclusion time:

21   20s).

22   *Peptide and Protein Identification* - Proteins were identified from RAW data files, with

23   trypsin specified as the protease, with one missed cleavage allowed and with fixed

24   modifications of carbamidomethyl cysteine and variable modifications of oxidation of

25   methionine (Peaks® Studio v8.5, Bioinformatics Solutions, Waterloo, Canada). Searches

1   were performed against the UniProt *Rattus Norvegicus* database

2   (www.uniprot.org/proteomes), with an FDR of 1%, ≥2 unique peptides per protein and a

3   confidence score >20. Protein network analysis was performed using the Search Tool for

4   Retrieval of Interacting Genes/Proteins (STRING), v11.0 (Szklarczyk et al., 2019), and

5   proteins were further classified using MatrisomeDB (Hynes and Naba, 2012) and the Protein

6   ANalysis THrough Evolutionary Relationships (PANTHER) Classification System (Mi et al.,

7   2013). The proteomic data have been deposited to the ProteomeXchange Consortium via the

8   PRIDE partner repository (Perez-Riverol et al., 2019) with the data set identifier PXD015928

9   and 10.6019/PXD015928.

10   *Calculation of protein turnover rates* – Peptides at each time point were identified using

11   ProLuCID (Xu et al., 2015) searching against a reverse-decoyed protein sequence database

12   (UniProt *Rattus Norvigicus*, reviewed, accessed 23/04/2018). Fixed modifications of

13   carbamidomethyl cysteine and ≤3 variable modifications of oxidation of methionine were

14   allowed. Tryptic, semi-tryptic, and non-tryptic peptides within a 15-ppm mass window

15   surrounding the candidate precursor mass were searched. Protein identification was

16   performed using DTASelect (v.2.1.4) (Cociorva et al., 2006), with ≤1% global peptide FDR

17   and ≥2 unique peptides per protein. Protein turnover rates and resulting half-lives were

18   calculated using custom software (ProTurn v2.1.05; http://proturn.heartproteome.org) as

19   previously described and validated (Lam et al., 2014, Lau et al., 2016, Lau et al., 2018, Wang

20   et al., 2014). Briefly, RAW files were converted into mzML format (ProteoWizard,

21   v3.0.11781) for input into ProTurn, along with DTAselect-filter text files for protein

22   identification. ProTurn parameters were as follows: area-under-curve integration width:

23   60 p.p.m., extracted ion chromatograph smoothing: Savitzky-Golay filter (Savitzky and

24   Golay, 1964) over 7 data points. Non-steady state curve fitting was used to account for the

25   initial delay in uptake of ^{2}H, using a first-order kinetic curve to approximate the equilibration

1   of ^2H_2O in body water. Values of k_p and p_{ss} were inputted from the resultant curve fitting of

2   ^2H enrichment in serum samples. To control against false positive identifications, only

3   peptides that were explicitly identified in ≥4 data points were accepted for the calculation of

4   protein turnover. The 'Allow Peptide Modification' option was selected to include any

5   identified post-translationally modified peptides in kinetic curve-fitting, and peptide

6   isotopomer time series were included if R^2≥0.8 or standard error of estimate (S.E) ≤0.05

7   (Lam et al., 2014). Protein-level turnover rate is reported as the median and median absolute

8   deviation of the turnover rate constants of each accepted unique constituent peptide, from

9   which protein half-life can be calculated assuming a first order reaction (Lau et al., 2018).

10   For some proteins of interest, particularly in the IFM, automated calculation of turnover rates

11   was unsuccessful, due to unsuccessful automated identification of isotopomer peaks. In these

12   cases, turnover rate constants were calculated manually, using isotopomer peak height to

13   calculate the relative abundance of M_0 as a function of time (Thermo Xcalibur v2.2), and

14   fitting first order kinetic curves to estimate k (GraphPad Prism v8.0.2). As the labelling

15   pattern of each peptide is dependent on the number of available labelling sites (N), unlabelled

16   relative abundance of the 0th isotopomer (a), as well as the plateau level of enrichment of

17   deuterium (p_{ss}); these values were used to calculate the plateau values of the 0th isotopomer

18   (A_0) which occurs when the peptide is fully labelled. N was calculated from the literature

19   (Lam et al., 2014, Commerford et al., 1983). a was calculated from the peptide sequence and

20   natural abundance of heavy isotopes of carbon, nitrogen, oxygen and sulphur (Lam et al.,

21   2014). p_{ss} was calculated from the serum enrichment as detailed above. The following

22   equation was then used to calculate the plateau of A_0:

23   $$A_{0,PLATEAU} = a(1 - p_{ss})^N$$

1   Previous work demonstrates this accurately predicts the plateau measured experimentally

2   (Lam et al., 2014), therefore, for curve fitting calculations the plateau was constrained to the

3   calculated value for each peptide. To assess the degree of differences in curve fitting

4   performed by automated and manual approaches, k values were calculated using both

5   approaches for 10 peptides. Resulting k values differed by an average of 23%. This method

6   does not allow for direct comparison between manual and automated calculations of k, due to

7   differences in curve fitting method, but does allow differences in peptide k values between

8   IFM and FM to be assessed, when both are calculated manually.

9   *Statistical Analysis* – When ≥3 peptides were identified corresponding to a particular protein,

10   statistical differences in turnover rate constants in tendon phases were assessed using paired

11   t-tests, Wilcoxon matched pairs tests, or Mann-Whitney tests, with $p < 0.05$ (GraphPad Prism,

12   v8.2). The statistical test chosen was dependent on whether data were normally distributed,

13   which was assessed with Kolmogorov-Smirnov tests, and whether the same peptides were

14   identified in tendon phases, which allowed for paired statistical tests.

15

16

17

18   **Abbreviations:** Ambic, Ammonium Bicarbonate; COMP, cartilage oligomeric matrix

19   protein; DTT dithiothreitol; ECM, extracellular matrix; FDR, false discovery rate; FM,

20   fascicular matrix; FSR, fractional synthesis rate; GC-MS, gas chromatography-mass

21   spectrometry; GuHCl, Guanidine hydrochloride; IFM, interfascicular matrix; LC-MS/MS,

22   liquid chromatography-tandem mass spectrometry; TFA, Trifluoroacetic acid.

3   **References:**

4   ASHRAF KHARAZ, Y., ZAMBOULIS, D., SANDERS, K., COMERFORD, E., CLEGG, P.
5   & PEFFERS, M. 2017. Comparison between chaotropic and detergent-based sample
6   preparation workflow in tendon for mass spectrometry analysis. *Proteomics,* 17**,**
7   1700018-n/a.
8   BABRAJ, J. A., CUTHBERTSON, D. J. R., SMITH, K., LANGBERG, H., MILLER, B.,
9   KROGSGAARD, M. R., KJAER, M. & RENNIE, M. J. 2005. Collagen synthesis in
10   human musculoskeletal tissues and skin. *American Journal of Physiology:*
11   *Endocrinology and Metabolism,* 289**,** E864-E869.
12   BECHSHØFT, C. L., SCHJERLING, P., BORNØ, A. & HOLM, L. 2017. Existence of life-
13   time stable proteins in mature rats—Dating of proteins' age by repeated short-term
14   exposure to labeled amino acids throughout age. *PLOS ONE,* 12**,** e0185605.
15   CHAUDHURY, C., MEHNAZ, S., ROBINSON, J. M., HAYTON, W. L., PEARL, D. K.,
16   ROOPENIAN, D. C. & ANDERSON, C. L. 2003. The Major Histocompatibility
17   Complex–related Fc Receptor for IgG (FcRn) Binds Albumin and Prolongs Its
18   Lifespan. *The Journal of Experimental Medicine,* 197**,** 315-322.
19   COCIORVA, D., L. TABB, D. & YATES, J. R. 2006. Validation of Tandem Mass
20   Spectrometry Database Search Results Using DTASelect. *Current Protocols in*
21   *Bioinformatics,* 16**,** 13.4.1-13.4.14.
22   COMMERFORD, S. L., CARSTEN, A. L. & CRONKITE, E. P. 1983. The Distribution of
23   Tritium among the Amino Acids of Proteins Obtained from Mice Exposed to Tritiated
24   Water. *Radiation Research,* 94**,** 151-155.
25   CONNIZZO, B. K., YANNASCOLI, S. M. & SOSLOWSKY, L. J. 2013. Structure-function
26   relationships of postnatal tendon development: a parallel to healing. *Matrix Biology,*
27   32**,** 106-16.
28   CULAV, E. M., CLARK, C. H. & MERRILEES, M. J. 1999. Connective Tissues: Matrix
29   Composition and Its Relevance to Physical Therapy. *Physical Therapy,* 79**,** 308-319.
30   GODINHO, M. S. C., THORPE, C. T., GREENWALD, S. E. & SCREEN, H. R. C. 2017.
31   Elastin is Localised to the Interfascicular Matrix of Energy Storing Tendons and
32   Becomes Increasingly Disorganised With Ageing. *Scientific Reports,* 7**,** 9713.
33   GUMUCIO, J. P., SUGG, K. B. & MENDIAS, C. L. 2015. TGF-β Superfamily Signaling in
34   Muscle and Tendon Adaptation to Resistance Exercise. *Exercise and Sport Sciences*
35   *Reviews,* 43**,** 93-99.
36   HEINEMEIER, K. M., SCHJERLING, P., HEINEMEIER, J., MAGNUSSON, S. P. &
37   KJAER, M. 2013. Lack of tissue renewal in human adult Achilles tendon is revealed
38   by nuclear bomb 14C. *FASEB Journal,* 27**,** 2074-2079.
39   HEINEMEIER, K. M., SCHJERLING, P., HEINEMEIER, J., MØLLER, M. B.,
40   KROGSGAARD, M. R., GRUM-SCHWENSEN, T., PETERSEN, M. M. & KJAER,
41   M. 2016. Radiocarbon dating reveals minimal collagen turnover in both healthy and
42   osteoarthritic human cartilage. *Science Translational Medicine,* 8**,** 346ra90-346ra90.
43   HSUEH, M.-F., ÖNNERFJORD, P., BOLOGNESI, M. P., EASLEY, M. E. & KRAUS, V.
44   B. 2019. Analysis of "old" proteins unmasks dynamic gradient of cartilage turnover in
45   human limbs. *Science Advances,* 5**,** eaax3203.

1 HUMPHREY, J. D., DUFRESNE, E. R. & SCHWARTZ, M. A. 2014. Mechanotransduction
2   and extracellular matrix homeostasis. *Nature reviews. Molecular cell biology,* 15**,**
3   802-812.
4 HYNES, R. O. & NABA, A. 2012. Overview of the matrisome--an inventory of extracellular
5   matrix constituents and functions. *Cold Spring Harb Perspect Biol,* 4**,** a004903.
6 JEFFAY, H. 1960. The Metabolism of Serum Proteins: III. Kinetics of serum protein
7   metabolism during growth. *Journal of Biological Chemistry,* 235**,** 2352-2356.
8 KASTELIC, J., GALESKI, A. & BAER, E. 1978. The multicomposite structure of tendon.
9   *Connect Tissue Res,* 6**,** 11-23.
10 KATSMA, M. S., PATEL, S. H., ELDON, E., CORBELL, K. A., SHIMKUS, K. L.,
11   FLUCKEY, J. D. & CARROLL, C. C. 2017. The influence of chronic IL-6 exposure,
12   in vivo, on rat Achilles tendon extracellular matrix. *Cytokine,* 93**,** 10-14.
13 KHARAZ, Y. A., TEW, S. R., PEFFERS, M., CANTY-LAIRD, E. G. & COMERFORD, E.
14   2016. Proteomic differences between native and tissue-engineered tendon and
15   ligament. *Proteomics,* 16**,** 1547-1556.
16 KILKENNY, C., BROWNE, W. J., CUTHILL, I. C., EMERSON, M. & ALTMAN, D. G.
17   2010. Improving Bioscience Research Reporting: The ARRIVE Guidelines for
18   Reporting Animal Research. *PLOS Biology,* 8**,** e1000412.
19 KIM, T.-Y., WANG, D., KIM, A. K., LAU, E., LIN, A. J., LIEM, D. A., ZHANG, J., ZONG,
20   N. C., LAM, M. P. Y. & PING, P. 2012. Metabolic Labeling Reveals Proteome
21   Dynamics of Mouse Mitochondria. *Molecular & Cellular Proteomics,* 11**,** 1586-1594.
22 KOURY, M. J. 2016. Red blood cell production and kinetics. *Rossi's Principles of*
23   *Transfusion Medicine.*
24 KUO, C. K., PETERSEN, B. C. & TUAN, R. S. 2008. Spatiotemporal protein distribution of
25   TGF-βs, their receptors, and extracellular matrix molecules during embryonic tendon
26   development. *Developmental Dynamics,* 237**,** 1477-1489.
27 LAM, M. P. Y., WANG, D., LAU, E., LIEM, D. A., KIM, A. K., NG, D. C. M., LIANG, X.,
28   BLEAKLEY, B. J., LIU, C., TABARAKI, J. D., CADEIRAS, M., WANG, Y.,
29   DENG, M. C. & PING, P. 2014. Protein kinetic signatures of the remodeling heart
30   following isoproterenol stimulation. *The Journal of Clinical Investigation,* 124**,** 1734-
31   1744.
32 LAU, E., CAO, Q., LAM, M. P. Y., WANG, J., NG, D. C. M., BLEAKLEY, B. J., LEE, J.
33   M., LIEM, D. A., WANG, D., HERMJAKOB, H. & PING, P. 2018. Integrated omics
34   dissection of proteome dynamics during cardiac remodeling. *Nature Communications,*
35   9**,** 120.
36 LAU, E., CAO, Q., NG, D. C. M., BLEAKLEY, B. J., DINCER, T. U., BOT, B. M., WANG,
37   D., LIEM, D. A., LAM, M. P. Y., GE, J. & PING, P. 2016. A large dataset of protein
38   dynamics in the mammalian heart proteome. *Scientific Data,* 3**,** 160015.
39 MAROUDAS, A., BAYLISS, M. T., UCHITEL-KAUSHANSKY, N., SCHNEIDERMAN,
40   R. & GILAV, E. 1998. Aggrecan Turnover in Human Articular Cartilage: Use of
41   Aspartic Acid Racemization as a Marker of Molecular Age. *Archives of Biochemistry*
42   *and Biophysics,* 350**,** 61-71.
43 MCCABE, B. J., BEDERMAN, I. R., CRONIGER, C., MILLWARD, C., NORMENT, C. &
44   PREVIS, S. F. 2006. Reproducibility of gas chromatography–mass spectrometry
45   measurements of 2H labeling of water: Application for measuring body composition
46   in mice. *Analytical Biochemistry,* 350**,** 171-176.
47 MI, H., MURUGANUJAN, A., CASAGRANDE, J. T. & THOMAS, P. D. 2013. Large-scale
48   gene function analysis with the PANTHER classification system. *Nat. Protocols,* 8**,**
49   1551-1566.

MICHALSKI, A., DAMOC, E., HAUSCHILD, J.-P., LANGE, O., WIEGHAUS, A., MAKAROV, A., NAGARAJ, N., COX, J., MANN, M. & HORNING, S. 2011. Mass spectrometry-based proteomics using Q Exactive, a high-performance benchtop quadrupole Orbitrap mass spectrometer. *Molecular & cellular proteomics,* 10**,** M111.011015.

MILLER, B. F., OLESEN, J. L., HANSEN, M., DØSSING, S., CRAMERI, R. M., WELLING, R. J., LANGBERG, H., FLYVBJERG, A., KJAER, M., BABRAJ, J. A., SMITH, K. & RENNIE, M. J. 2005. Coordinated collagen and muscle protein synthesis in human patella tendon and quadriceps muscle after exercise. *Journal of Physiology,* 567**,** 1021-1033.

PEREZ-RIVEROL, Y., CSORDAS, A., BAI, J., BERNAL-LLINARES, M., HEWAPATHIRANA, S., KUNDU, D. J., INUGANTI, A., GRISS, J., MAYER, G., EISENACHER, M., PÉREZ, E., USZKOREIT, J., PFEUFFER, J., SACHSENBERG, T., YILMAZ, S., TIWARY, S., COX, J., AUDAIN, E., WALZER, M., JARNUCZAK, A. F., TERNENT, T., BRAZMA, A. & VIZCAÍNO, J. A. 2019. The PRIDE database and related tools and resources in 2019: improving support for quantification data. *Nucleic acids research,* 47**,** D442-D450.

POWERS, E. T., MORIMOTO, R. I., DILLIN, A., KELLY, J. W. & BALCH, W. E. 2009. Biological and Chemical Approaches to Diseases of Proteostasis Deficiency. *Annual Review of Biochemistry,* 78**,** 959-991.

ROBINSON, K. A., SUN, M., BARNUM, C. E., WEISS, S. N., HUEGEL, J., SHETYE, S. S., LIN, L., SAEZ, D., ADAMS, S. M., IOZZO, R. V., SOSLOWSKY, L. J. & BIRK, D. E. 2017. Decorin and biglycan are necessary for maintaining collagen fibril structure, fiber realignment, and mechanical properties of mature tendons. *Matrix Biology,* 64**,** 81-93.

RUSSO, V., MAURO, A., MARTELLI, A., DI GIACINTO, O., DI MARCANTONIO, L., NARDINOCCHI, D., BERARDINELLI, P. & BARBONI, B. 2015. Cellular and molecular maturation in fetal and adult ovine calcaneal tendons. *Journal of Anatomy,* 226**,** 126-142.

RYS, J. P., MONTEIRO, D. A. & ALLISTON, T. 2016. Mechanobiology of TGFβ signaling in the skeleton. *Matrix biology : journal of the International Society for Matrix Biology,* 52-54**,** 413-425.

SAVITZKY, A. & GOLAY, M. J. E. 1964. Smoothing and Differentiation of Data by Simplified Least Squares Procedures. *Analytical Chemistry,* 36**,** 1627-1639.

SCOTT, J. E. 1983. Connective tissues: the natural fibre-reinforced composite material. *Journal of the Royal Society of Medicine,* 76**,** 993-994.

SIVAN, S.-S., WACHTEL, E., TSITRON, E., SAKKEE, N., VAN DER HAM, F., DEGROOT, J., ROBERTS, S. & MAROUDAS, A. 2008. Collagen Turnover in Normal and Degenerate Human Intervertebral Discs as Determined by the Racemization of Aspartic Acid. *Journal of Biological Chemistry,* 283**,** 8796-8801.

SIVAN, S. S., TSITRON, E., WACHTEL, E., ROUGHLEY, P. J., SAKKEE, N., VAN DER HAM, F., DEGROOT, J., ROBERTS, S. & MAROUDAS, A. 2006. Aggrecan Turnover in Human Intervertebral Disc as Determined by the Racemization of Aspartic Acid. *Journal of Biological Chemistry,* 281**,** 13009-13014.

SMEETS, J. S. J., HORSTMAN, A. M. H., VLES, G. F., EMANS, P. J., GOESSENS, J. P. B., GIJSEN, A. P., VAN KRANENBURG, J. M. X. & VAN LOON, L. J. C. 2019. Protein synthesis rates of muscle, tendon, ligament, cartilage, and bone tissue in vivo in humans. *PLOS ONE,* 14**,** e0224745.

SÖDERSTEN, F., HULTENBY, K., HEINEGÅRD, D., JOHNSTON, C. & EKMAN, S. 2013. Immunolocalization of Collagens (I and III) and Cartilage Oligomeric Matrix

Protein in the Normal and Injured Equine Superficial Digital Flexor Tendon. *Connective Tissue Research,* 54**,** 62-69.

SPIESZ, E. M., THORPE, C. T., CHAUDHRY, S., RILEY, G. P., BIRCH, H. L., CLEGG, P. D. & SCREEN, H. R. 2015. Tendon extracellular matrix damage, degradation and inflammation in response to in vitro overload exercise. *Journal of orthopaedic research,* 33**,** 889-97.

SWOVICK, K., WELLE, K. A., HRYHORENKO, J. R., SELUANOV, A., GORBUNOVA, V. & GHAEMMAGHAMI, S. 2018. Cross-species Comparison of Proteome Turnover Kinetics. *Molecular & Cellular Proteomics,* 17**,** 580-591.

SZKLARCZYK, D., GABLE, A. L., LYON, D., JUNGE, A., WYDER, S., HUERTA-CEPAS, J., SIMONOVIC, M., DONCHEVA, N. T., MORRIS, J. H., BORK, P., JENSEN, L. J. & MERING, C. V. 2019. STRING v11: protein-protein association networks with increased coverage, supporting functional discovery in genome-wide experimental datasets. *Nucleic acids research,* 47**,** D607-D613.

TAVILL, A. S. 1972. The synthesis and degradation of liver-produced proteins. *Gut,* 13**,** 225-241.

THORPE, C. T., CHAUDHRY, S., LEI, II, VARONE, A., RILEY, G. P., BIRCH, H. L., CLEGG, P. D. & SCREEN, H. R. 2015a. Tendon overload results in alterations in cell shape and increased markers of inflammation and matrix degradation. *Scandinavian Journal of Medicine and Science in Sports,* 25**,** e381-91.

THORPE, C. T., GODINHO, M. S., RILEY, G. P., BIRCH, H. L., CLEGG, P. D. & SCREEN, H. R. 2015b. The interfascicular matrix enables fascicle sliding and recovery in tendon, and behaves more elastically in energy storing tendons. *Journal of the Mechanical Behavior of Biomedical Materials,* 52**,** 85-94.

THORPE, C. T., KARUNASEELAN, K. J., NG CHIENG HIN, J., RILEY, G. P., BIRCH, H. L., CLEGG, P. D. & SCREEN, H. R. C. 2016a. Distribution of proteins within different compartments of tendon varies according to tendon type. *Journal of Anatomy,* 229**,** 450-458.

THORPE, C. T., PEFFERS, M. J., SIMPSON, D., HALLIWELL, E., SCREEN, H. R. & CLEGG, P. D. 2016b. Anatomical heterogeneity of tendon: Fascicular and interfascicular tendon compartments have distinct proteomic composition. *Scientific Reports,* 6**,** 20455.

THORPE, C. T., RILEY, G. P., BIRCH, H. L., CLEGG, P. D. & SCREEN, H. R. 2016c. Fascicles and the interfascicular matrix show adaptation for fatigue resistance in energy storing tendons. *Acta Biomater,* 42**,** 308-15.

THORPE, C. T., STREETER, I., PINCHBECK, G. L., GOODSHIP, A. E., CLEGG, P. D. & BIRCH, H. L. 2010. Aspartic acid racemization and collagen degradation markers reveal an accumulation of damage in tendon collagen that is enhanced with aging. *Journal of Biological Chemistry,* 285**,** 15674-81.

THORPE, C. T., UDEZE, C. P., BIRCH, H. L., CLEGG, P. D. & SCREEN, H. R. 2012. Specialization of tendon mechanical properties results from interfascicular differences. *Journal of the Royal Society Interface,* 9**,** 3108-17.

VERZIJL, N., DEGROOT, J., THORPE, S. R., BANK, R. A., SHAW, J. N., LYONS, T. J., BIJLSMA, J. W. J., LAFEBER, F. P. J. G., BAYNES, J. W. & TEKOPPELE, J. M. 2000. Effect of Collagen Turnover on the Accumulation of Advanced Glycation End Products. *Journal of Biological Chemistry,* 275**,** 39027-39031.

WANG, D., LIEM, D. A., LAU, E., NG, D. C. M., BLEAKLEY, B. J., CADEIRAS, M., DENG, M. C., LAM, M. P. Y. & PING, P. 2014. Characterization of human plasma proteome dynamics using deuterium oxide. *Proteomics – Clinical Applications,* 8**,** 610-619.

1 WILLIAMSON, J. R., EDWARDS, A. V. G., VERANO-BRAGA, T., SCHWÄMMLE, V.,
2   KJELDSEN, F., JENSEN, O. N. & LARSEN, M. R. 2016. High-performance hybrid
3   Orbitrap mass spectrometers for quantitative proteome analysis: Observations and
4   implications. *Proteomics,* 16**,** 907-914.
5 XU, T., PARK, S. K., VENABLE, J. D., WOHLSCHLEGEL, J. A., DIEDRICH, J. K.,
6   COCIORVA, D., LU, B., LIAO, L., HEWEL, J., HAN, X., WONG, C. C. L.,
7   FONSLOW, B., DELAHUNTY, C., GAO, Y., SHAH, H. & YATES, J. R. 2015.
8   ProLuCID: An improved SEQUEST-like algorithm with enhanced sensitivity and
9   specificity. *Journal of Proteomics,* 129**,** 16-24.
10 ZAMBOULIS, D. E., THORPE, C. T., BIRCH, H. L., SCREEN, H. R. & CLEGG, P. D.
11   2018. Pre- and post-natal development of the tendon inter-fascicular matrix and
12   fascicles in the equine superficial digital flexor tendon and common digital extensor
13   tendon. *Osteoarthritis and Cartilage,* 26**,** S403-S404.

14

15 **Supplementary Information**

16 Supplementary Table 1. All proteins and corresponding peptides identified in whole tendon

17 samples

18 Supplementary Table 2. All proteins and corresponding peptides identified in the

19 interfascicular matrix

20 Supplementary Table 3. All proteins and corresponding peptides identified in the fascicular

21 matrix

22 Source Table 1. Enrichment of serum water as measured by GC-MS.

23 Source Table 2. ProTurn output for whole tendon. hl tab contains protein half-life

24 information organized by peptide sequence and hl-data tab contains isotopomer relative

25 abundance at each time point

26 Source Table 3. ProTurn output for FM. hl tab contains protein half-life information

27 organized by peptide sequence and hl-data tab contains isotopomer relative abundance at

28 each time point

1   Source Table 4. ProTurn output for IFM. hl tab contains protein half-life information

2   organized by peptide sequence and hl-data tab contains isotopomer relative abundance at

3   each time point

4   Supplementary Figure 1. **Protein-protein interaction map of proteins identified in whole**

5   **tendon**, **interfascicular matrix and fascicular matrix**. Unconnected nodes were removed to

6   provide clarity of the interactome. The total cluster was built with STRING allowing for

7   experimentally verified and predicted protein-protein interactions at high confidence levels

8   (0.700). Line thickness indicates the strength of supporting data

9

10